Thermodynamic Stability of Immiscible Polymer Blends†

Sabine Vanhee, Ronald Koningsveld, and Hugo Berghmans*

Laboratory of Polymer Research, Catholic University Leuven, Belgium

Karel Šolc

Physics Department, Central Michigan University, Mt. Pleasant, Michigan 48859

Walter H. Stockmayer

Chemistry Department, Dartmouth College, Hanover, New Hampshire 03755

Received October 28, 1999; Revised Manuscript Received February 22, 2000

ABSTRACT: Calculations based on an extended Flory−Huggins−Staverman model demonstrate that miscibility gaps in virtually immiscible blends may encompass a complex pattern of metastable and unstable equilibria that differ little in Gibbs free energy. Examples are given that demonstrate the development of near immiscibility by sideways coalescence of upper-critical and lower-critical gaps upon an increase of the chain lengths of the constituents. The mechanisms of merging are discussed, as well as the effect of chain-length distribution and copolymer composition. The conceivable occurrence of nonstable equilibria may lead to a change in physical properties of immiscible blends with time, here called thermodynamic aging of the second kind.

Introduction

Many high−polymer blends exist in which mutual miscibility is negligibly small. The Flory−Huggins−Staverman model[1−6] in its simplest form suggests that a reduction of the (average) chain lengths in the two constituents will bring about partial, and eventually complete miscibility of either the lower (LC) or upper (UC) consolute type. Simultaneous occurrence of LC and UC behavior calls for a slightly extended temperature dependence of the interaction function,[7,8] and it is conceivable that virtually immiscible polymer blends present a state arising from the coalescence of UC and LC miscibility gaps upon an increase of the chain lengths; Figure 1 illustrates this. The coalescence may occur in several ways, some of which may involve complex patterns of metastable equilibria that differ very little in Gibbs free energy from the eventual stable equilibrium.[9] Consequently, in polymer blend processing they might play a confusing role, and some further study of possible coalescence mechanisms would not seem to be superfluous.

Restricting the discussion to strictly binary homopolymer blends for the moment, we can distinguish two main processes: merging of miscibility gaps by coalescence of their critical points (c−c) or by sideways coalescence. The latter may take place in two fashions: either by one of the critical points moving toward the flank of the other gap (c−nc), or by two flanks touching one another (nc−nc), the abbreviation "nc" standing for "noncritical". In one of the previous papers,[9] it was found that the merging mechanisms for c−nc and nc−nc coalescence differed markedly, and it is one of the objectives of the present paper to further explore this difference. Since any actual polymer is characterized by molecular polydispersity (chain length distribution and/or copolymer composition), we also include the results of some calculations which focus on these features. This work forms part of the Ph.D. Thesis of S.V.[10]

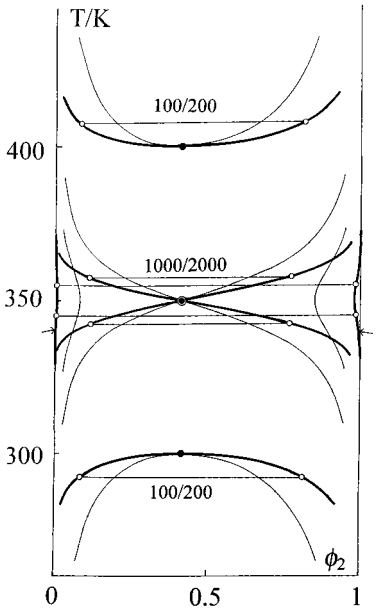

Figure 1. Coalescence of binary UC and LC miscibility gaps via a homogeneous double critical point (double circle) at $m_1/m_2 = 1000/2000$, calculated with eqs 1−4 and 7. $\chi_1 = 1.4571 \times 10^{-3}$, $\chi_2 = 5.2456 \times 10^{-6}$, and $T_0 = 350$ K. LC and UC phase boundaries are shown for 100/200. Those for 2500/5000 are indicated by arrows and show virtual immiscibility but for some dissolution of polymer 1 in the polymer 2-rich phase in a small temperature niche at 350 K. Key: binodals, heavy curves; spinodals, light curves; critical points, filled circles; tie lines, horizontal lines connecting conjugate phases (open circles).

Flory−Huggins−Staverman (FHS) Model

Two-liquid-phase equilibria in blends consisting of two polymers can be calculated with the FHS expression for ΔG, the Gibbs free energy of mixing the $\sum n_{1i}$ mole of

† Affectionately dedicated to prof. Karel Dušek of Prague on the occasion of his 70th birthday.

10.1021/ma9918102 CCC: $19.00
Published on Web 04/15/2000

polymer 1 with the $\sum n_{2j}$ mole of polymer 2. The model is known to supply at least a qualitatively correct description of the phase behavior[11,12] but can be made almost quantitative if the Van-Laar parameter g in the interaction function Γ is allowed to depend on concentration and temperature and, sometimes molar mass[7,13−15]

$$\Delta G/NRT = \sum(\varphi_{1i}/m_{1i})ln\ \varphi_{1i} + \sum(\varphi_{2j}/m_{2j})\ln\ \varphi_{2j} + \Gamma \quad (1)$$

$$\Gamma = g(T,\varphi_2)\varphi_1\varphi_2$$

where N = number of basic volume units (BVU) in the system in mole, $\varphi_{kl} = (n_{kl}m_{kl})/\{\sum(n_{1i}m_{1i} + \sum(n_{2j}m_{2j})\} = n_{kl}m_{kl}/N$ = volume fraction of component l in polymer k (k = 1,2; l = running index i or j), $\varphi_k = \sum\varphi_{kl}$ = volume fraction of whole polymer k, and m_{kl} = "chain length", the number of BVUs occupied by chain molecule l in polymer k.

The spinodal is defined by

$$J_s = 1/(m_{w1}\varphi_1) + 1/(m_{w2}\varphi_2) + (\partial^2\Gamma/\partial\varphi_2 2)_{p,T} = 0 \quad (2)$$

and the liquid−liquid critical state by

$$J_c = \xi_{w1}/(m_{w1}\varphi_1^2) - \xi_{w2}/(m_{w2}\varphi_2^2) + (\partial^3\Gamma/\partial\varphi_2^3)_{p,T} = 0 \quad (3)$$

$$(\xi_{wk} = m_{zk}/m_{wk})$$

where m_{wk} and m_{zk} are the weight- and z-average chain lengths of polymer k.

Chemical potentials $\Delta\mu_{kl}$ are given by

$$\Delta\mu_{1i}/(m_{1i}RT) = (\ln\ \varphi_{1i})/m_{1i} + 1/m_{1i} - \varphi_1/m_{n1} - \varphi_2/m_{n2} + \zeta_1\varphi_2^2 \quad (4)$$

where m_{nk} is the number-average chain length of polymer k, and

$$\zeta_1 = g + \varphi_1(\partial g/\partial\varphi_1)$$

($\Delta\mu_{2j}$ is obtained upon exchange of indices).

Equations 2−4 can be used to calculate two-dimensional (quasi-)binary phase diagrams for partially miscible blends of two polymers.[16] If g does not depend on composition

$$g = \zeta_1 = \zeta_2 \equiv \chi \quad (5)$$

and we have the FHS model in its simplest form with

$$\chi = \chi_s + h/T \quad (6)$$

where χ_s and h are entropic and enthalpic contributions, respectively. Either LC or UC behavior can be covered and are defined by the sign of h ($h < 0$ or $h > 0$, respectively).[9]

The description of simultaneous occurrence of LC and UC calls for a slightly extended temperature function of χ.[7−9,17] The simple symmetric expression in (7) serves a useful purpose for qualitative comparisons[8]

$$\chi = \chi_1 + \chi_2(T - T_0)^2 \quad (7)$$

where χ_1 and χ_2 are constants. Figure 1 illustrates some applications of eqs 2−4 and 7 for strictly binary blends. Before proceeding further, a note on multiple critical point (CP) notation is called for.

Qualification of Multiple Critical Points

The simplest case of multiple CPs seems to occur on critical lines (CL) passing through a three-dimensional space. For instance, in ternary condensed systems (two independent composition variables + temperature) with simple interactions, a double critical point, whether heterogeneous or homogeneous, appears as a local temperature extremum of the CL running through the triangular prism of the composition-temperature space. It is the perturbation of temperature that invokes the process of merging two single CPs on a binodal into a double CP, and the CL direction at the double CP is entirely contained within the constant temperature plane. This kind of double CP was discussed more than 100 years ago by Korteweg[18] and further elaborated on by Korteweg and Schreinemakers,[19] by Tompa,[12] and, more recently, in our work.[9]

However, van der Waals and Kohnstamm,[20] as well as Korteweg,[21] have already made it clear that multiple CPs can be defined in a more general context, with the composition and temperature of the above case replaced by other variables. Specifically, they examined in great detail multiple CPs in binary compressible systems, produced in the composition−volume plane by changes in temperature. In this broader view also the well-known case[22] of merging lower and upper CPs, induced by changing the molar mass of the polymer in some binary solvent/polymer systems, is recognized as a homogeneous double CP.[9]

Since each of the above examples describes physically different phenomena existing under different circumstances, it is advisable to characterize the arising multiple CPs by some qualifier. The latter certainly should contain the variable (boldfaced) whose change is responsible for the process of CP merging. However, for a complete characterization it should also include the space in which the merging process proceeds. Using this notation, we might qualify Korteweg's case[18] by ***T****xx*, van der Waals' case[20,21] by ***T****Vx*, and Zeman and Patterson's LC/UC example[22] by ***M****Tx*, where x stands for a generalized composition variable, T is the temperature, V is the volume, and M is the polymer molar mass.

Thus, the coalescence of upper and lower CPs in Figure 1 results in an ***M****Tx homogeneous double critical point* (HODCP) (or *homogeneous double plait point*, as it used to be called in the van der Waals school.[19,20,23] It is indicated by a double circle. In a HODCP two CPs of identical stability coalesce (both stable in Figure 1). In Korteweg's terminology a heterogeneous double critical (plait) point (HEDCP) marks the merging of two CPs of different stability. The various abbreviations defined above are summarized in Table 1.

Sideways Coalescence in Strictly Binary Blends

As long as the concentration dependence of g is ignored, as in (5), coalescence will always follow the pattern of Figure 1. Sideways coalescence, if occurring at all, indicates concentration dependence of g, the various molecular reasons for which can be covered qualitatively by a polynomial the order of which does not usually need to exceed 2[24]

$$g = g_0 + g_1\varphi_2 + g_2\varphi_2^2 \quad (8)$$

Table 1. Abbreviations

LC	lower-critical miscibility
UC	upper-critical miscibility
CL	critical line
CP	critical point
CPC	cloud point curve
c−c	merging of miscibility gaps by coalescence of two CPs
nc	noncritical
c−nc	merging by coalescence of a CP with the flank of another miscibility gap
nc−nc	sideways merging of two miscibility gaps
FHS	Flory−Huggins−Staverman
HODCP	homogeneous double CP
HEDCP	heterogeneous double CP
NSM	nonstable merging within a stable miscibility gap

Table 2. Interaction-Parameter Values for Figures 2−8 and 11−13

Figure	x	g_{0s} × 10²	g_{0h} × 10²/K	g_{1s} × 10²	g_{1h} × 10²/K	g_{2s} × 10²	g_{2h} × 10²/K
2	1	0.5188	−63.37	−0.6595	126.7	0.2672	0
4	1.2	0.4058	−39.01	−0.6257	129.9	0.2875	−13.75
5	1.4	0.3251	−21.62	−0.6015	132.2	0.3020	−23.57
6	1.6	0.2646	−8.572	−0.5834	133.9	0.3128	−30.94
7	1.8	0.2175	1.577	−0.5693	135.2	0.3213	−36.67
3	2	0.1798	9.696	−0.5581	136.3	0.3281	−41.26
8	4	0.01039	46.23	−0.5074	141.1	0.3585	−61.89
11	2	0.1798	9.696	−0.5581	136.3	0.3281	−41.26
12	1	0.5188	−63.37	−0.6595	126.7	0.2672	0
13	1	χ_{eff}		−0.3522	34.56	0.1135	−46.09

where each of the coefficients may depend on temperature

$$g_i = g_{is} + g_{ih}/T \tag{9}$$

We consider binaries with $m_2 = xm_1$ where $x \geq 1$. Phases will be met that are either stable, metastable, or unstable,[9,25] and we shall adopt the term nonstable for equilibria involving one or both of the latter two. The preceding paper was concerned with x values of 1 and 2 only. It gives an extensive discussion of the relevant phase equilibria, as well as details of the calculation procedure[9] (see also ref 10). The numerical values of the constants used in the calculations and in Figures 2−8 and 11−13, are listed in Table 2. They have been chosen to center the T-axis at or near 320 K.

In the symmetric case, $x = 1$, merging of the UC and LC gaps occurs via nc−nc coalescence which is preceded by the formation of nonstable crescent-shaped binodals within each of the two gaps (Figure 2a). Figure 2b schematically shows the tie lines which indicate that the two crescents are conjugate with one another. The extrema of the crescents, though located on the spinodal, are not critical points but coexist with the cusps.[18,19] When the two gaps touch there is a nonvariant three-phase equilibrium among three liquid phases. Such equilibria are indicated by a horizontal line indicating the phase compositions by triangular symbols.

When the two gaps penetrate one another (Figure 2c), there are two three-phase lines between which the outer branches of the two crescents have become stable. Upon an increase of m_1 the inner branches will come to coalesce in a singular point S on the right-hand branch of the LC spinodal (nonstable merging; NSM) as is seen in Figure 2d, and the pattern changes abruptly (Figure 2e). Upon further increase of m_1 the two inner spinodal branches move closer together until, at $m_1 = 1057.67$, a HODCP of the ***M****Tx* type is created at their contact point (Figure 2f), and the pattern again changes abruptly. At $m_1 > 1057.67$ this HODCP splits up into two instable

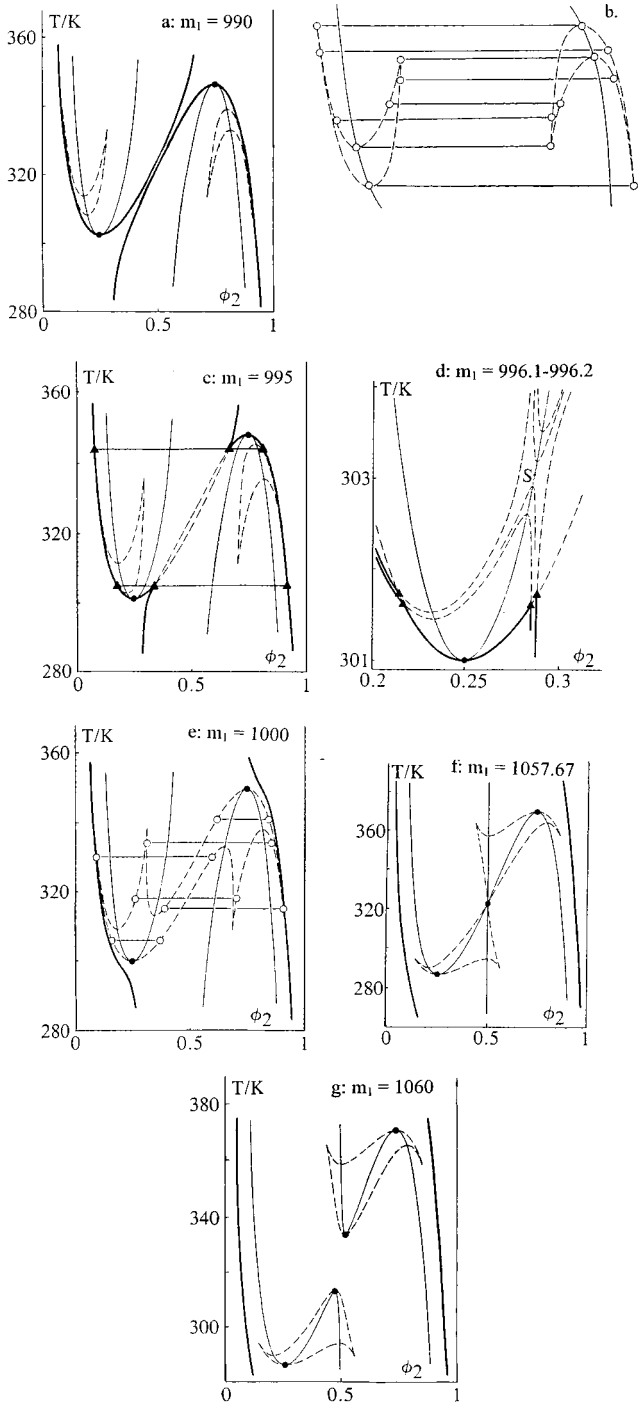

Figure 2. Sideways merging of an LC and a UC miscibility gap in a strictly binary polymer blend, calculated with eqs 1−4, 8, and 9 with parameter values listed in Table 1. Value of m_1 indicated; $m_2 = xm_1$, $x = 1$. Symbols as in Figure 1. Dashed curves: nonstable binodals.

CPs, each on a double-sigmoidal self-contained binodal (Figure 2g). The two bisigmoids finally disappear in two HEDCPs where instable and metastable CPs merge.[18,19]

For $x = 2$ the mechanism is considerably different. Merging occurs via c−nc coalescence, the UC binodal forming a shoulder when the LC gap approaches. When contact is made the shoulder has a horizontal tangent and the LC's CP has become a critical end point (critical phase in equilibrium with another phase[20,23]) (Figure 3a). It is seen in Figure 3b that the horizontal tie line in Figure 3a is in fact is a degenerated three-phase line, two of the phases just being critically identical. In

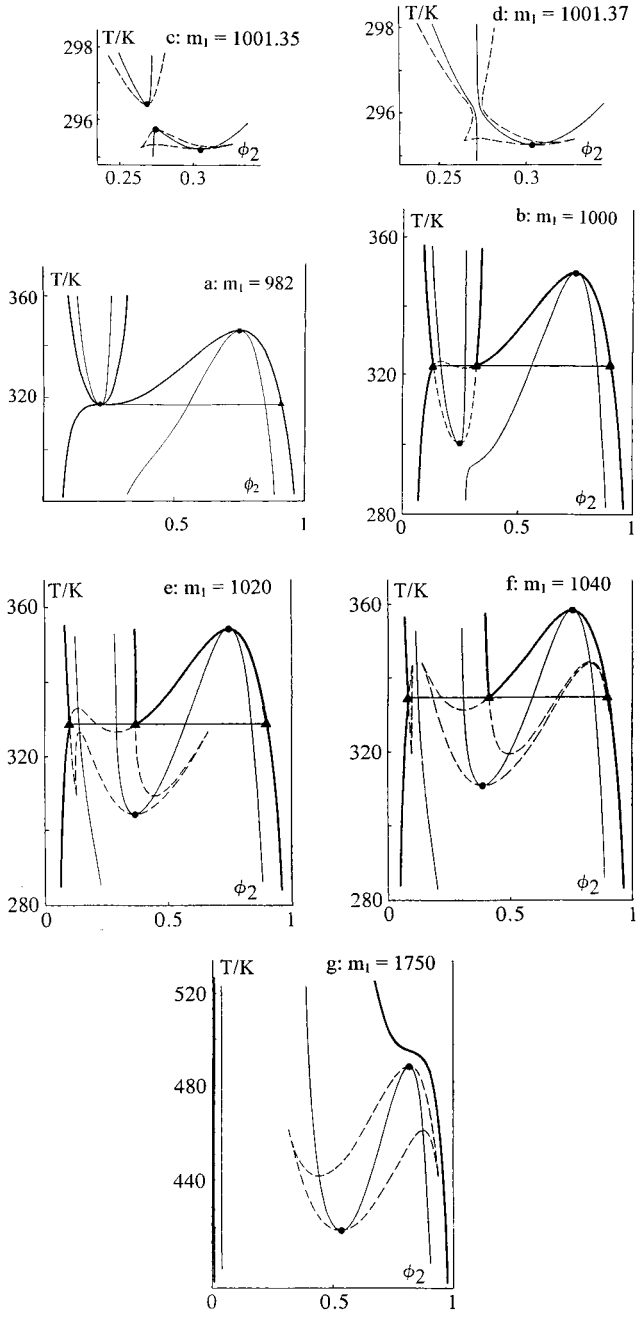

Figure 3. As in Figure 2, $x = 2$.

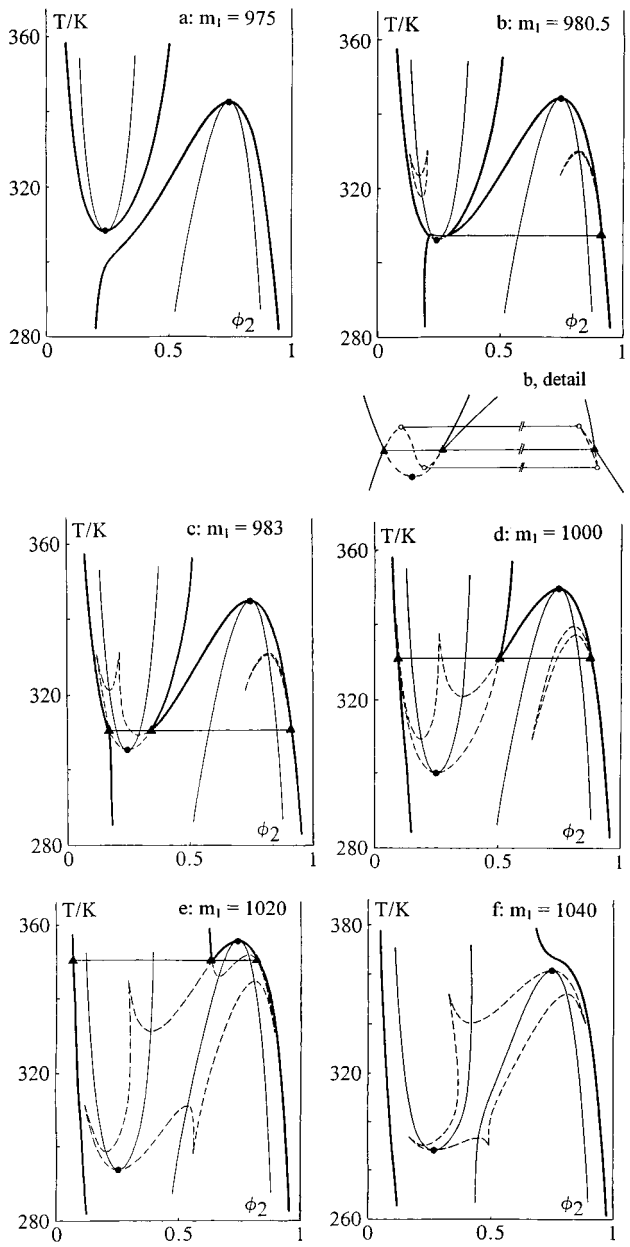

Figure 4. As in Figure 2, $x = 1.2$.

Figure 3b, the UC spinodal develops a shoulder which changes via a HEDCP into the sigmoidal shape going with a nonstable bisigmoid-type binodal (Figure 3c), the lhs. CP of which merges with the LC CP in a HODCP. Further increase of m_1 gives rise to a boot-shaped nonstable binodal, whose noncritical maximum between sole and heel moves to higher temperatures when m_1 increases (Figure 3d,e). Finally, it hits the l.h. maximum in the nonstable extension of the UC binodal and two new cusps arise above the three-phase line (Figure 3f). Later on, the stable CP on the UC gap becomes metastable (Figure 3g). The mechanism for $x = 2$ is thus seen to be less complex than that for $x = 1$ and to involve NSMs of a different type.

To understand better the differences between the patterns of $x = 1$ and $x = 2$, we now study a few intermediate values. At $x = 1.2$ (Figure 4a) the approach of the two gaps is already seen to go without the "rubbing-shoulder" nc−nc behavior of the symmetrical system (Figure 2a), the UC gap developing a shoulder as with $x = 2$. As a consequence there will again be one three-phase line only. The follow-up is different here, however. While there are no nonstable crescents being formed at $x = 2$, they occur at $x = 1.2$ in addition to the formation of the three-phase line via a critical end point (Figure 4b). The descending l.h. crescent comes to interfere with the maximum of the nonstable extension of the UC binodal (see Figure 4b, schematic inset) which leads to the diagram of Figure 4c,d. Next, NSM takes place on the l.h. branch of the UC spinodal, resulting in Figure 4e. After the CP of the UC binodal has become metastable via a critical end point situation, we obtain Figure 4f. A split-up via a HODCP, analogous to that in Figure 2e,f occurs next.

At $x = 1.4$, no nonstable crescents develop, but two cusps are formed on the sharp maximum of the nonstable extension of the UC binodal (Figure 5a,b), together with the coexisting crescent within the UC gap. The minimum between the two l.h. cusps deepens, NSM

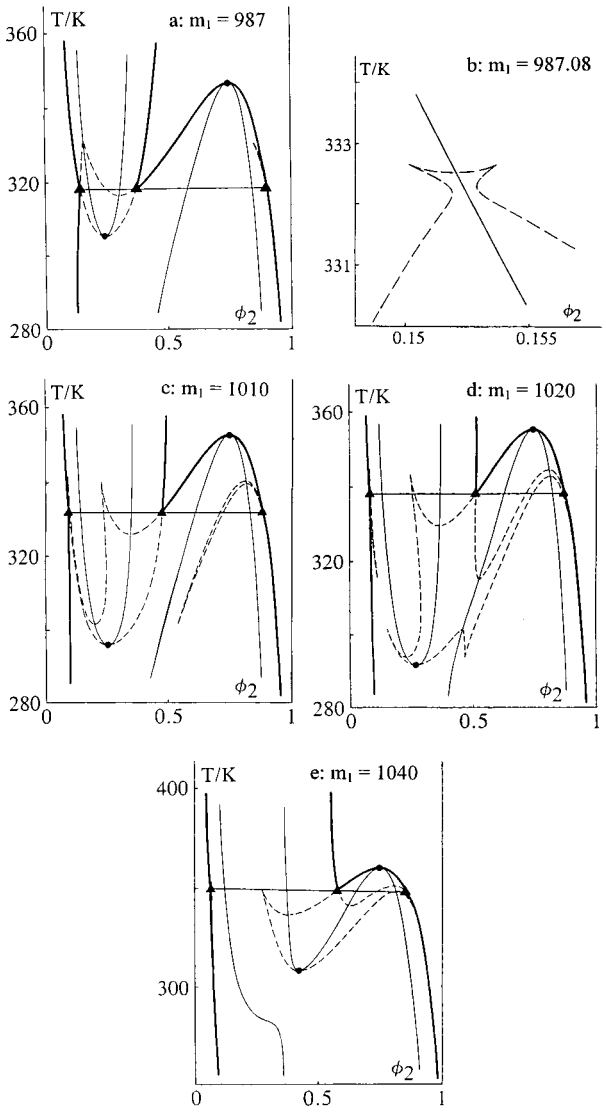

Figure 5. As in Figure 2, $x = 1.4$.

takes place on the l.h. branch of the UC spinodal (Figure 5c,d), and after a HODCP splitting of the spinodals, we obtain the situation of Figure 5e, which is familiar now.

With $x = 1.6$, we have a new phenomenon. After passing the critical end point, we note in Figure 6a the coming into existence of a nonstable ellipsoid on the l.h. branch of the LC spinodal, with a shallow conjugate crescent within the UC gap. Increasing m_1 we observe the maximum of the ellipsoid to coincide with the maximum in the UC binodal to form two cusps coexisting with the two maxima on the other side of the diagram, arising from the coalescence of the two cusps there on the rhs of Figure 6a. The minimum of the ellipsoid has moved to lower temperature. Figure 6b illustrates the situation. Next, merging of the nonstable l.h. branches of LC gap and ellipsoid occur, followed by spinodal splitting via a HODCP, after which the diagram of Figure 6c is obtained. Finally, we reach a situation quite analogous to that in Figure 5e.

For $x = 1.8$ the ellipsoid comes into existence at lower temperature than with $x = 1.6$ (Figure 7a). There is merging of the nonstable l.h. branches of LC binodal and ellipsoid (Figure 7b). After passing through the now familiar HODCP state, we see the emergence of the boot shape described for $x = 2$ (Figure 7c).

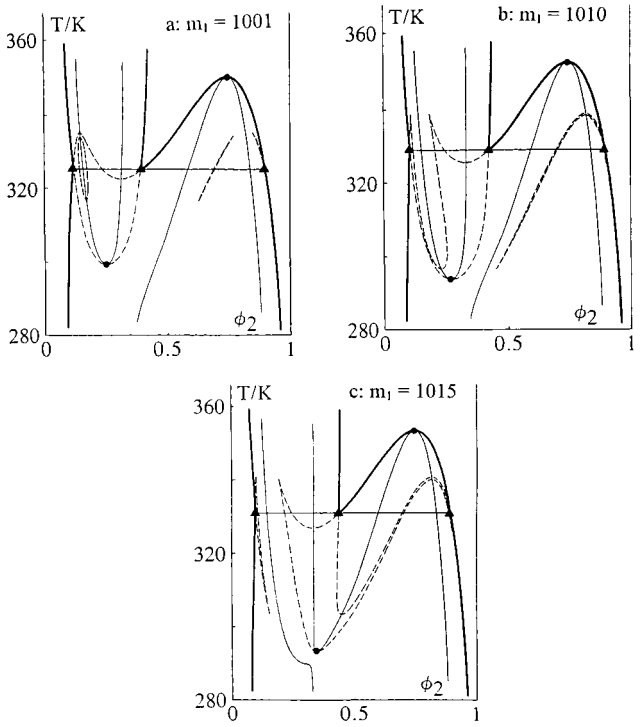

Figure 6. As in Figure 2, $x = 1.6$

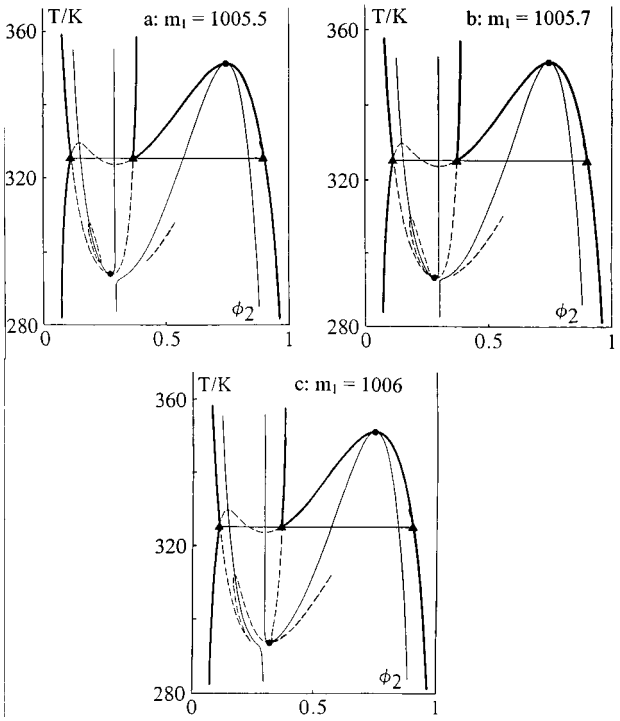

Figure 7. As in Figure 2, $x = 1.8$.

For $x > 2$ there are no further essential differences. The nonstable crescent on the l.h. branch of the UC spinodal now already occurs when the LC binodal is still some temperature distance away from the UC gap. Figure 8 gives an example for $x = 4$. For the rest the mechanism of $x = 2$ is followed.

Experimental Indications for Sideways Merging

As far as the authors are aware, sideways merging of miscibility gaps in polymer blends has not explicitly been reported. There is an indication in the literature, however, that seems to point to the possible existence

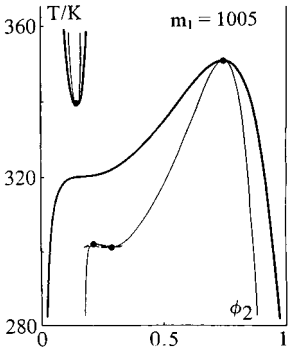

Figure 8. As in Figure 2, $x = 4$.

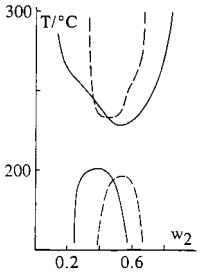

Figure 9. Partial miscibility in the system PS/carboxylated poly(2,6-dimethyl-1,4-phenylene oxide) showing separate UC and LC miscibility gaps and their change in shape upon a variation of the carboxyl content of the PPO: full curves, 8.0 mol %; dashed curves, 10.3 mol %. Data by Cong et al.[26] Weight fraction of CPPO: w_2.

of such phase behavior. Cong et al.[26] studied the system polystyrene/carboxylated poly(2,6-dimethyl-1,4-phenylene oxide); their data are represented by the curves in Figure 9. It is seen that the shape and location of the LC and UC gaps with respect to each other change with the degree of carboxylation of the second constituent. Proof of sideways merging is not supplied by the data, but nevertheless they leave this possibility open for samples of higher average molar masses than used in the experiments.

For two reasons, this experimental example is not quite representative for the phase diagrams presented above. First, the data refer to unfractionated polymers that must have a sizable molar-mass distribution. Second, the changes in the phase diagrams are not brought about by a variation in chain length but by a chemical change of the second constituent. The chemically modified product could be considered as a copolymer of changing chemical composition. We shall therefore in the next section analyze the effect of molecular polydispersity of both kinds.

Effect of Molecular Polydispersity

Molar-Mass Distribution. The first step in investigations of the effect of a distribution of chain lengths consists of replacing the single component polymer by a mixture of two homologues differing in chain length.[7,23] We consider blends of a single-component polymer 1 ($m_1 = 990$) and a binary polymer 2 that consists of two components in equal weights, and we keep the weight-average chain length m_{w2} constant while, at constant ratio $x = m_{w2}/m_1$, drawing the two chain lengths in polymer 2 gradually apart. The latter manoeuver causes the ratios m_w/m_n ($=\xi_n$) and m_z/m_w ($=\xi_w$) to become larger.

The most striking difference between the strictly binary phase diagrams of Figures 2-8 and the *quasi-binary* phase diagrams that are presented in Figures 10 and 11 is the fact that the heavy curves in these diagrams do not represent binodals (locus of coexisting-

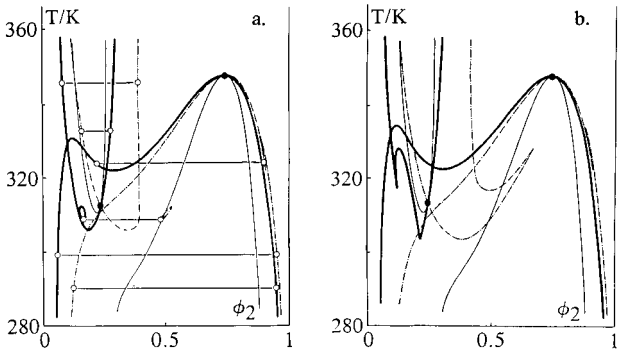

Figure 10. Sideways coalescence of LC and UC gaps in a quasi-binary polymer blend containing a single-component polymer 1 ($m_1 = 990$) and a binary polymer 2 ($m_{w2} = xm_1$, $x = 2$). Key: heavy curves, cloud-point curves; dash−dot curves, shadow curves; light curves, spinodals; filled circles, critical points. Projected tie lines: horizontal lines connecting cloud-point and shadow phases (open circles). (a) $\xi_{n2} = 1.095$, $\xi_{w2} = 1.087$; (b) $\xi_{n2} = 1.118$, $\xi_{w2} = 1.106$.

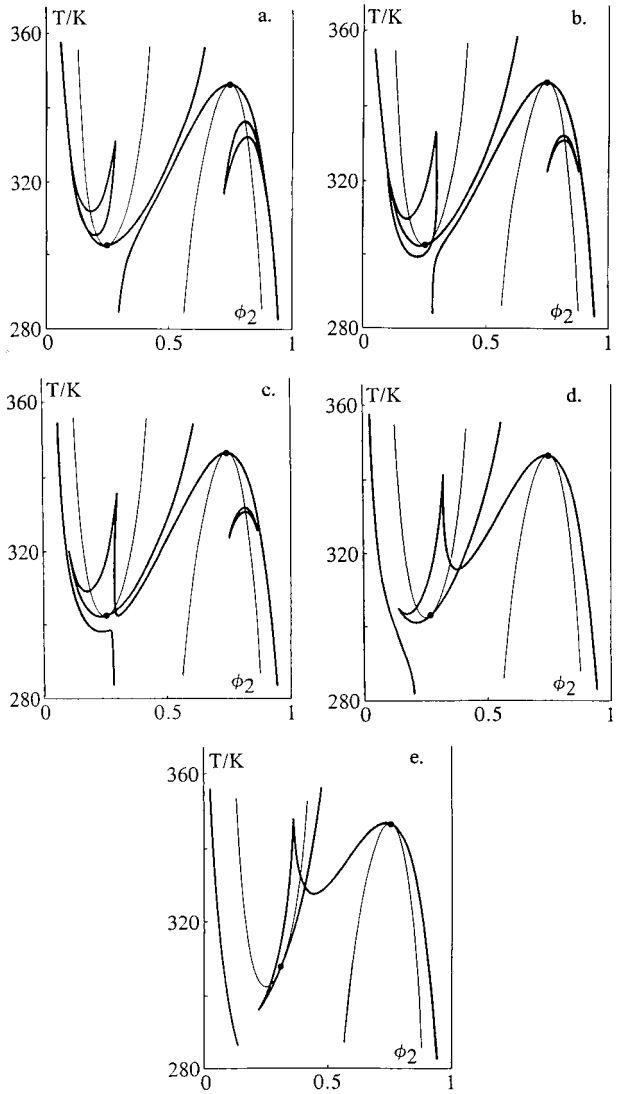

Figure 11. As in Figure 10 (shadow curves not shown), $x = 1$: (a) $\xi_{n2} = 1.0101$, $\xi_{w2} = 1.0100$; (b) $\xi_{n2} = 1.030$, $\xi_{w2} = 1.029$; (c) $\xi_{n2} = 1.033$, $\xi_{w2} = 1.032$; (d) $\xi_{n2} = 1.099$, $\xi_{w2} = 1.090$; (e) $\xi_{n2} = 1.33$, $\xi_{w2} = 1.25$.

phase compositions) but are so-called *cloud-point curves* (CPC) the extremum of which is in general not a CP. Any cloud point on a CPC coexists with a phase that is on the verge of appearing but whose composition is outside the plane of drawing. The latter composition can be projected onto the plane of the quasi-binary phase diagram and loci of such projections are found in Figure 10 as dash−dot, so-called *shadow curves*.[7,10,23]

At $x = 2$ we note in Figure 10a,b that, although we have the general c−nc pattern of Figure 3, nonstable equilibria now occur in the form of an ellipsoidal CPC on the lhs, coexisting with shadow phases in another ellipsoid on the rhs, a phenomenon not seen with $x = 2$ in Figure 3. The slightest increase of the width of the distribution causes it to disappear.

At $x = 1$ merging starts in a similar fashion as in Figure 2 (Figure 11a). For the sake of clarity no shadow curves are shown. Again, the slightest widening of the chain-length distribution changes the pattern considerably, and the merging takes place in a peculiar fashion, resembling c−nc coalescence, and leaving in the beginning a peculiar narrow channel of miscibility (Figure 11b,c). The final shape is reminiscent of c−nc merging with $x = 2$ in Figure 3 (Figure 11d,e).

Copolymer Composition. To check the effect of the copolymer composition we consider strictly binary blends containing a homopolymer 1 and a statistical copolymer 2. The interaction function (eq 6) must be adapted to account for the fact that we have now three types of molecular contacts in the system in stead of two. This feature was first studied by Simha and Branson[27] and was later also investigated by Stockmayer et al.[28] and by others. For the present purpose it is sufficient to realize that the Simha−Branson derivation yields an expression for an effective quantity χ_{eff} given by

$$\chi_{\text{eff}} = x_\alpha \chi_{1\alpha} + x_\beta \chi_{1\beta} - x_\alpha x_\beta \chi_{\alpha\beta} \qquad (10)$$

where x_α and x_β are the segment fractions of α and β units in the copolymer and the three χ's represent the three types of contacts. Since we need the concentration dependence of g to obtain sideways coalescence at all, we use (8), replacing g_0 by χ_{eff}. The influence of the chemical composition can be mimicked by comparing phase diagrams calculated for different values of χ_{eff} while keeping the other parameters constant.

Figure 12a−c was calculated in this way for a strictly binary blend with $m_1 = 1000$, $x = 1$, and three slightly different values of χ_{eff}. The effect is seen to be large.

Conclusions

The ever present chain-length distributions in polymer blends appear only to add to the complexity of phase behavior in systems with sideways merging LC and UC miscibility gaps. Such virtually immiscible blends must by the present calculations be expected to show great subtlety and variety. Small variations in copolymer composition further complicate the issue.

The question may be raised whether the material presented here could have any practical consequence. One point can be made safely: the present considerations strongly indicate that the thermodynamic stability of supposedly immiscible polymer blends may not be as obviously simple as one might think. Figure 13 shows the $\Delta G(\varphi_2)$ curve for the system of Figure 6b at 325 K. There are four equilibrium situations possible for a mixture of the two polymers after having been

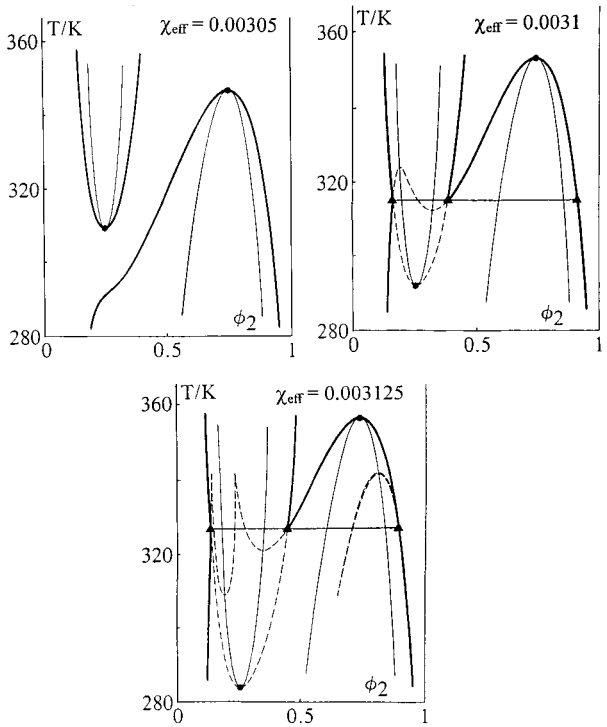

Figure 12. Sideways coalescence in a strictly binary polymer blend containing a homopolymer 1 ($m_1 = 1000$) and a statistical copolymer 2 ($m_2 = 1000$). Calculated with eqs 1−4 and 8 with g_0 replaced by χ_{eff}, for indicated values of the latter. Symbols as in Figure 2.

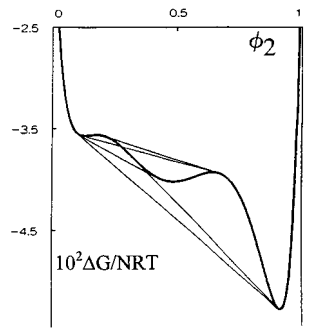

Figure 13. $\Delta G/NRT$ against φ_2 for the system of Figure 6b at 325 K.

brought together in an extruder. The top double tangent refers to two unstable phases that would each be subject to spinodal decomposition. The original value of ΔG for the unmixed polymers being zero, and the viscosities involved being enormous, it is not inconceivable that the blend will in one pass through the extruder not even reach the ΔG value going with the top tangent. Even if so, the next level would be the second tangent from the top which refers to nonstable equilibrium between an unstable and a metastable phase. The two tangents following next refer to metastable equilibrium that might remain established because of the kinetic hindrances. It is only the bottom tangent that defines the stable equilibrium. It would seem quite conceivable that the blend, in the course of preparation and reprocessing might decrease its ΔG value in the course of time and consequently change its physical properties.

We suggest the term *thermodynamic aging of the second kind* for such a physical aging process. Thermodynamic aging of the first kind has been described earlier[29] and refers to immiscible blends of two molecularly polydisperse polymers. In such cases theory pre-

dicts equilibrium to involve partial dissolution of the shorter chains in one of the constituent polymers into the phase, rich in the other constituent. Strictly binary blends do not exhibit thermodynamic aging of the first kind, the second kind is here seen to be open to blends of any polydispersity, provided their state of immiscibility is the result of sideways merging of UC and LC miscibility gaps.

Acknowledgment. This research was financed by the IWONL through a fellowship for S.V. The project was also supported by the Fund for Scientific Research, Flanders, and the Inter-University Poles of Attraction, Belgian State, Prime Minister's Office for Scientific Research, Technical and Cultural Affairs (IUAP IV, P4/11). Thanks are further due to Mr. Frank Meeussen for his assistance in the preparation of the manuscript.

References and Notes

(1) Staverman, A. J.; Van Santen, J. H. *Recl. Trav. Chim.* **1941**, *60*, 76.
(2) Staverman, A. J. *Recl. Trav. Chim.* **1941**, *60*, 640.
(3) Huggins, M. L. *J. Chem. Phys.* **1941**, *9*, 440.
(4) Huggins, M. L. *Ann. N. Y. Acad. Sci.* **1942**, *43*, 1.
(5) Flory, P. J. *J. Chem. Phys.* **1941**, *9*, 660.
(6) Flory, P. J. *J. Chem. Phys.* **1942**, *10*, 51; **1944**, *12*, 114.
(7) Koningsveld, R. *Adv. Coll. Interface Sci.* **1968**, *2*, 151.
(8) Šolc, K, Stockmayer, W. H.; Lipson; J. E. G.; Koningsveld, R. *Multiphase Macro-molecular Systems*; Culbertson, B. M., Ed.; Plenum: New York, 1989; p 5.
(9) Šolc, K.; Koningsveld, R. *J. Phys. Chem.* **1992**, *96*, 4056.
(10) Vanhee, S. Ph.D. Thesis, Leuven 1994.
(11) Flory, P. J. *Principles of Polymer Chemistry*; Cornell University Press: Ithaca, NY, 1953.
(12) Tompa, H. *Polymer Solutions*; Butterworth: London, 1956.
(13) Nies, E. Ph.D. Thesis, Antwerp 1983.
(14) Nies, E.; Koningsveld, R.; Kleintjens, L. A. *Prog. Colloid Polym. Sci.* **1985**, *71*, 2.
(15) Van Opstal, L.; Koningsveld, R. *Polymer* **1992**, *33*, 3433, 3445.
(16) Šolc, K.; Koningsveld, R. *Collect. Czech Chem. Commun.* **1995**, *60*, 1689.
(17) Qian, C.; Mumby, S. J.; Eichinger, B. E. *J. Polym. Sci., Part B: Polym. Phys.* **1991**, *29*, 635.
(18) Korteweg, D. J. *Sitzungsber. Kais. Akad. Wiss., Math.-Naturwiss. Kl.* **1889**, *98, 2. Abt. A*, 1154.
(19) Korteweg, D. J.; Schreinemakers, F. A. H. *K. Acad. Wet. Amsterdam* **1911**, *20*, 476, 490.
(20) van der Waals, J. D.; Kohnstamm, Ph. D. *Lehrbuch der Thermodynamik*; Barth: Leipzig, Germany, 1912; Vol. II.
(21) Korteweg, D. J. *Versl. Kon. Nederl. Akad. Wetensch.* 1902/03, *XI*, 515.
(22) Zeman, L.; Patterson, D. *J. Phys. Chem.* **1972**, *76*, 1214.
(23) Koningsveld, R.; Stockmayer, W. H.; Nies, E. *Polymer Phase Diagrams*; Oxford University Press: in press.
(24) Šolc, K.; Kleintjens, L. A.; Koningsveld, R. *Macromolecules* **1984**, *17*, 573.
(25) Horst, R. *J. Phys. Chem. B* **1998**, *102*, 3243.
(26) Cong, G.; Huang, Y.; MacKnight, W. J.; Karasz, F. E. *Macromolecules* **1986**, *19*, 2765.
(27) Simha, R.; Branson, H. *J. Chem. Phys.* **1944**, *12*, 253.
(28) Stockmayer, W. H.; Moore, L. D., Jr.; Fixman, M.; Epstein, B. N. *J. Polym. Sci.* **1955**, *16*, 517.
(29) Koningsveld, R.; Šolc, K.; MacKnight, W. J. *Macromolecules* **1993**, *26*, 6676.

MA9918102